

Tidal components along the north of Oman Gulf and Persian Gulf

Maryam Soyuf Jahromi^{1*}

^{1*} Assistant Professor of physical oceanography, Department of Nonliving Resources of Atmosphere and Ocean, Faculty of Marine Science and Technology, University of Hormozgan, Bandar Abbas, Iran; soyuffjahromi@yahoo.com.au

ARTICLE INFO

Article History:

Received: 05 Oct. 2023

Accepted: 16 Jan. 2024

Keywords:

Tides

Tidal constituents

Persian Gulf

t-tide Library

Matlab

ABSTRACT

This study concentrates on the 61 tidal constituents of 17 stations on the north of Oman Gulf (OG), Strait of Hormuz (SH) and Persian Gulf (PG). Five-years tidal data (2014-2018, 30-minutes intervals) was achieved by Iran National Cartographic Center to calculate mean levels of stations. Then, t_tide library was used to calculate 61 tidal constituents by 95% of confidence in Matlab for 2018 data. Then, they sorted by the magnitude of the amplitude to express the most significant ones in each stations. Results shows that the mean levels of the northwest and northeast of PG are mirror images. Although the major diurnal and semidiurnal tidal constituents of 11 stations are M_2 , K_1 , S_2 and O_1 , by changes in order of importance; in 6 stations, N_2 constituent is more important than O_1 . These exceptions go back to the stations of SH and northwest of PG, which shows the importance of the SH bending and the shallowing of the northwest of PG. Moreover, the top ten components of all stations are not 10 unique components and they include 21 components. Due to the Form factor, F, all the studied stations are mainly mixed semidiurnal type. The predicted t-tide tides show small errors compare with the original ones. The results also showed that the range and components of harmonic astronomical tides are influenced by local geography. On the head of PG, the Emam Khomeini's tides is sharp due to the shallow water, and the semidiurnal components (S_2 and N_2) are much stronger than the diurnal components (O_1 and P_1). The Pol Port's tides is effected by narrowing of SH. Therefore, in some ports, non-tidal parameters such as geographical shape or shallow water are effective while considering astronomical components of moon and sun.

1. Introduction

For thousands of years, tides have been so important economically and scientifically that have entered our everyday language, and a saying like "time and tide wait for no one" is a clear example. Tide is important for navigation and ocean mixing. In the vertical mixing of coastal waters with a horizontal scale of 10 km or less and a time interval shorter than 24 hours, tides plays an effective role [1]. Tides can suspend bed sediments even in deep oceans. In addition, it can cause internal waves on seamounts, continental slopes, and midoceanic ridges, which dissipate lethal energy. In tidal history, real oceanic tides are considered stable because of their close association with astronomical motions [2]. Since the earth's crust is elastic and rotates counter-clockwise around its axis [3], due to the difference in the gravity of the moon, sun, and other celestial bodies, the earth's crust is bent under the influence of the tidal potential [4] and as a result, the

ocean fluctuates semidiurnal, diurnal or with other frequencies.

In classical analysis, it is customary to decompose the recorded tidal observations into its components, and the tidal signal is modeled as a finite sum of a sinusoidal terms with specific frequencies, related to astronomical parameters. These parameters are related to many factors such as latitude, the north deviation of the moon/sun from the equator, the hour angle of the moon/sun, the deviation of the earth's rotation axis, the inclination of the earth's rotation axis with respect to the stars, the rotation of the plane of the celestial sphere, and the temporal variations of the elliptic inclination of the earth's rotation in the plane of the celestial sphere and the angle of the moon's ellipse in a plane depend on the plane of the celestial sphere [5-7]. These processes cause changes in tidal potential.

Fourier analysis is used to determine frequencies of tidal spectrum. The spectrum does not look like the oceanic wave spectrum. Oceanic waves have all

possible frequencies by a continuous spectrum while tides have precise discontinuous frequencies. It consists of discrete lines related to astronomical motions and harbor properties. Doodson (1922) [8] expanded tidal potential as Fourier series using the cleverly chosen frequencies, leads to an elegant decomposition of tidal constituents into groups with similar frequencies and spatial variability. Doodson's expansion included 399 constituents, of which 100 are long period, 160 are daily, 115 are twice per day, and 14 are thrice per day. Although most constituents had very small amplitudes, but the amplitude accuracy of 10^{-3} of the largest term requires at least 39 frequencies be determined.

The Standard list of tidal constituents was prepared by Mr. Bernard Simon of SHOM (Service hydrographique et océanographique de la marine) and Cdr John Page of the UKHO (The United Kingdom Hydrographic Office) on behalf of IHO (The International Hydrographic Organization) Tidal Committee, now it is called the Tide, Water Level and Current Working Group (TWCWG) [9]. By evolving tides at diverse rates, there is not sometimes any apparent relationship to astronomical force [10-13] and may change major diurnal and semidiurnal tides (eg. Eastern Pacific [14], Gulf of Maine [15], North Atlantic [16-17], China [18-19] and Japan [20]).

Non-tidal variability introduces large errors into the calculated amplitudes and phases of weaker tidal constituents. The weaker tides have amplitudes smaller than variability at the same frequency due to the other processes such as wind set up and currents near the tide gauge.

This research is planned to examine the tidal constituents on major ports along the north Oman Gulf (here after, OG) towards Persian Gulf (here after, PG). These basins have different tidal variability that may affects their tidal constituents.

The tidal circulation in PG was modeled by a homogeneous two dimensional shallow-water model with free surface and forced by seven tidal components at its southern boundary [21]. The model accurately reproduced the tidal phase and amplitude observed at 42 tidal gauges in the region. This accuracy was attributed to the presence of seven components which are able to interact nonlinearly. The amphidromic points were also well positioned by the model due to a proper choice of bathymetry. The tidal currents could be strong in the Straits of Hormuz (here after, SH) and in shallow areas; thus they would have an effect of the hydrology of the region. The residual currents were weak so that they were negligible for the large-scale circulation on long periods. Finally, the sea-surface elevation forecast by the model was in close agreement with *insitu* measurements of pressure, performed during the GOGP99 experiment [21].

Akbari et al., (2016) [22] were also simulated three tidal semidiurnal (M_2 , S_2 , K_2) and diurnal (K_1 , O_1 , Q_1)

amplitudes in PG and OG by FVCOM (Finite Volume Coastal Ocean Model). They clearly showed that the different characteristics of PG and OG. The semidiurnal constituents (M_2 , S_2 , K_2) has two amphidromic points while diurnal constituents (K_1 , O_1 , and Q_1) had only one amphidromic points on PG. None of them had amphidromic points on OG. The tide simultaneously happens on OG is unlike PG. The model showed that tides of PG is a constant wave with two semi-diurnal and one diurnal amphidromic point. But tides of OG and the Arabian Sea is a progressive wave that moves on surfaces. The most important semidiurnal and diurnal components in the entire domain was M_2 and k_1 [22].

As can be seen, there are few near-shore studies of various components on PG, OG and SH. This study examines the components (61 constituents) near the coast of PG and OG by a library function named t-tide. These components will be checked on different ports of area to see if they have non-tidal effects by their geometric position.

2. Materials and Methods

2.1. Study area

The study area (48-62°E, 22-30°N) is a coastal area along the north of OG and PG with their connection through SH. Coastlines of the study area achieved by Iranian Army Geographic Agency as a shape file with the resolution of 30 seconds and plotted by ArcGIS 9.2 [23] software (Figure 1). The study area divided into three parts: OG, SH and PG. PG also divided into two parts of northeast and northwest because of its geometric shape.

OG (also named Macran or Mecran in native language), is a kind of strait (not an actual gulf) that connects the Arabian Sea to the SH which then runs to PG. OG is linked from three sides to the land by depths less than 1000 m and to the open ocean on the other side by depths more than 3000 m [24].

PG itself is a semi-enclosed marginal sea by total area of 240,000 km² [25], completely located on a continental shelf and downhill of OG. PG is a water catchment area drawn from the northwest to the southeast. Its length is 990 km while the width differs from 56 km to 338 km by the mean depth of 35 meters [1]. Its morphology is asymmetrical and the coastal slope is more relaxed on the southern coast than the northern coast [25]. SH, a curved waterway, separates Iran's plateau from the Arabian Peninsula and links the PG waters to OG and the Indian Ocean (here after, IO). Since PG is located on the subtropical high-pressure-zone, it is characterized by low precipitation (0.07–0.1 m yr⁻¹ [26]) and high aridity, resulting high evaporation rates (above 2 m yr⁻¹ [27]; 1.4–2.1 m yr⁻¹ [28-29]), 1.5 meters of the surface in a year [30-33]) by seasonal Sea Surface Temperature (SST) changes [34]. High precipitation is rare in this area [35-36]. This makes PG as one of the most saline water of the world (36.6 to

40.6 [37]) because of high evaporation, less precipitation (less than 5 mm yr^{-1}) and less river inflow

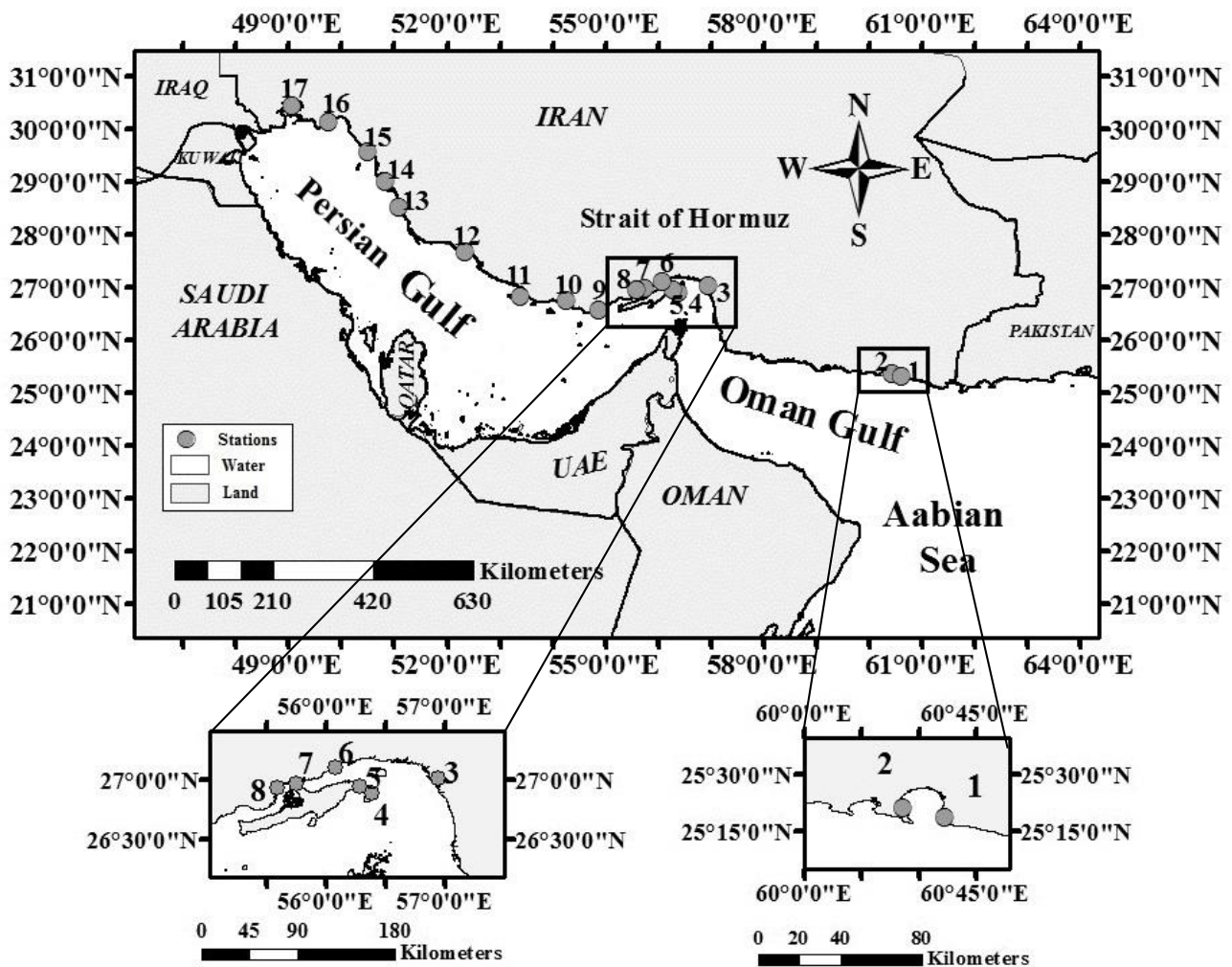


Figure 1. The study area. Oman Gulf (OG), Strait of Hormuz (SH), and Persian Gulf (PG). Gray circle marks are tidal stations (Table 1). The map is generated by ArcGIS [23] and the coastlines are achieved by Iranian Army Geographic Agency.

(0.15 m yr^{-1} [29]). The salinity is higher near the southern part [1, 32]. The saline water forms a very dense water especially in early November, when the air temperature decreases and wind speed increases [37]. It can also make some mesoscale eddies by the diameters less than 50 meters [38]. The dense flow of PG travels to OG by seasonal changes [39-43] to depths of 150 to 350 meters [44] through the south of SH. It makes changes on the thermoclines of OG [45] and deepen it to 1200 meters [46]. The less saline water of OG enters PG through the north of SH and replaces the outflow of PG [44, 47] for equilibrium [48]. This water is warmer than surrounding waters [49-50].

Tides are complicated on PG and OG. Tides of PG co-oscillate with SH while tides of OG co-oscillate with the Arabian Sea [1] and they make different tidal conditions in PG, SH and OG [51]. Due to the complex geometric shape of the coastline, tides of PG fluctuates [52] and has potential extracted energy [53]. PG has a diurnal and semidiurnal fluctuations, which initially emitted energy from SH into OG [52]. The tidal patterns of PG change from semidiurnal to diurnal tides [1]. The tidal range is

more than one meter (three meters on the head of PG and one meter on the other parts) [54]. The dimensions of PG are such that the resonance amplification of the tides occur [1]. Therefore, PG tides are kinds of standing tidal waves [1] by different amphidromic points (nodes) of constituents. There are two amphidromic points for semidiurnal constituents (M_2 and S_2) and one amphidromic point for diurnal constituents (K_1 and O_1) [55-57]. The magnitude of M_2 is approximately 0.3 m to 0.5 m at each point of PG and its maximum is 0.8 m to 0.9 m at the head of PG and near SH. The magnitude of S_2 is about 30% of M_2 . The O_1 amphidromic point is in the north of Bahrain by the amplitude of about 0.3 m. The K_1 amphidromic point is near Bahrain by the amplitude of about 0.5 m on the head of PG [52]. Near the amphidromic points of the diurnal components (K_1 and O_1), where the diurnal tidal component is zero, it is the semidiurnal tidal type, and near the amphidromic points of the semidiurnal components (M_2 and S_2), tides is diurnal [21]. According to the information of the National Oceanic and Atmospheric Administration (NOAA) organization, the next effective recorded

components of the world are M_4 , N_2 , M_6 , MK_3 , S_4 , MN_4 , NU_2 , S_6 , MU_2 , $2N_2$. If PG and GO assumed as a unit basin, the longitudinal axis of the area must be considered as a channel with two gaps that may affect the independent tides, where the phase of the tide-generating force would depend upon the longitudinal direction of this unified basin [51].

2.2. The tidal data

Seventeen tidal stations were chosen on the north of OG, SH and PG (Figure 1). Two stations were located on OG (Station 1-2: Chabahar and Konarak), six stations are located on SH (Station 3-8: Bandzak, Larak, Bahman Port, Shahid Rajaei Port, Pol Port, and Khamir Port), four stations are located on the northeast of PG (Station 9-12: Lengeh Port, Charak Port, Lavan, and Taheri) and five stations are located on the northwest of PG (Station 13-17: Ameri Port, Bushehr, Genaveh Port, Butaheri, and Emam Khomeini Port), respectively. Table 1 shows the location of station.

Table 1. Tidal stations of the study along the northern coasts of OG, SH and PG

Basin	Station No. and Name	Longitude (°E)	Latitude (°N)
Oman Gulf (OG)	St. 1 Chabahar	60.6165619	25.3133678
	St. 2 Konarak	60.4328461	25.3552799
Strait of Hormuz	St. 3 Bandzak	56.9478073	27.0106392
	St. 4 Larak	56.3899193	26.8866272
	St. 5 Bahman Port	56.2816048	26.9481812
	St. 6 Shahid Rajaei Port	56.0767288	27.1017857
	St. 7 Pol Port	55.7470436	26.9729309
	St. 8 Khamir Port	55.5921097	26.9380035
North-East	St. 9 Lengeh Port	54.8850327	26.5486584
	St. 10 Charak Port	54.2820778	26.7251301
	St. 11 Lavan	53.4027261	26.8010977
	St. 12 Taheri	52.3495789	27.6610126
Persian Gulf (PG)	St. 13 Ameri Port	51.0914993	28.5146675
	St. 14 Bushehr	50.8374710	28.9896507
	St. 15 Genaveh Port	50.5117722	29.5597763
	St. 16 Butaheri	49.7747765	30.1060658
	St. 17 Emam Khomeini Port	49.0720100	30.4219837

Tidal information was achieved by Iran National Cartographic Center, Water Management and Tidal Affairs [58] by every 30 minutes' interval for five continuous available years (January 1, 2014 to December 31, 2018). Mean Level (ML) achieved by the average of these five years for each station. Since long-term data are affected by the harbor modifications [59-64] or changes of internal tide [65-66], only one-year data (2018) was used to analysis tidal constituents.

2.3. Data Analysis

The tidal signal is simulated as the sum of finite sets of sinusoids at specific frequencies related to astronomical parameters. Since each tidal constituent is assumed to be a harmonic function and couched in the cosine term, it can be rewrite in a vectorization form of a time series (Eq. 1) as formulated by [67]:

$$\varepsilon(t) = \sum_{i=0}^n H_i' \cos(E_i' - g_i) \quad (1)$$

Consequently, the number of parameters is related to the number of used (significant) constituents. The `t_tide` Matlab library allows the calculation of various tidal constituents by the projection of series of harmonic functions on the data. `t_tide` library was written first on January 2011 [68], and then revised [69]. It is available online [70] and used in other recent studies [71-75].

In this research, the first 61 significant constituents are used. Therefore, a set of programs has been rewritten in MATLAB [76] to perform the harmonic analysis for each station in 2018. This library is based on the Fortran based tidal packages developed for the Canadian government [77]. Outputs of the `t_tide` library consists of 61 tidal constituents as SSA, MSM, MM, MSF, MF, ALP1, 2Q1, SIG1, Q1, RHO1, O1, TAU1, BET1, NO1, CHI1, PI1, P1, K1, PHI1, THE1, J1, SO1, OO1, UPS1, OQ2, EPS2, 2N2, MU2, N2, NU2, M2, MKS2, LDA2, L2, S2, K2, MSN2, ETA2, MO3, M3, SO3, MK3, SK3, MN4, M4, SN4, MS4, MK4, S4, SK4, 2MK5, 2SK5, 2MN6, M6, 2MS6, 2MK6, 2SM6, MSK6, 3MK7, M8, M10 with frequencies ranging from 0.0015 (MM constituents) to 0.3220 (M8 constituents) cycles per hour [69] (hereafter cph). It was also used the shallow water constituents [78-79] for OG and PG which was not previously used on the documents of this area.

Frequencies, amplitudes and errors for each constituent on each station was calculated by the 95% of confidence intervals (here after 95% CI). Then, tidal constituents sorted by the magnitude of the amplitude to expresses the most significant constituents of the stations.

New tides were also made according to the extracted 61-components to calculate the difference between the predicted tides and the original ones [58] for seven selected stations (Station 1: Chabahar, Station 4: Larak, Station 8: Khamir Port, Station 9: Lengeh Port, Station 12: Taheri, Station 14: Bushehr, Station 17: Emam Khomeini Port). Since Mean level on PG have shown monthly [80] and seasonally [81] changes, therefore, the predicted water levels by components are corrected by the mean achieved water level of the time series of 2014-2018 for each station.

Form factor (F) was also calculated to classify stations according to the nature of tides as Eq. 2 [82-84]:

$$F = \frac{K_1 + O_1}{M_2 + S_2} \quad (2)$$

where the symbols of the constituents indicate their respective amplitudes. Type of tide was determined as diurnal, semidiurnal and mixed by F factor (Table 2).

Table 2: The classification of tides due to the form factor values, F [82-84].

Value of F	Type of tide
0-0.25	Semidiurnal
0.25-1.5	Mixed, mainly semidiurnal
1.5-3	Mixed, mainly diurnal
>3	Diurnal

3. Results and Discussion

3.1. The tidal times series

Figure 2 shows the mean value of stations (2014-2018). It is obvious that Mean Level (ML) is not constant; it is less on OG, becomes higher in SH, fall down in the northeast of PG and again rises on the northwest of PG. The highest values are referred to Emam Khomeini Port (2.94 m) located on the northwest of PG (Station 17) and Pol Port (2.54 m) located on the SH (Station 7). Emam Khomeini Port is a shallow port, and in other studies such as [85], its tidal range was reported large in compared with other regions of PG. Pol Port, which is the shortest distance between Iran's southern coast line and Qeshm Island, experiences high values of tides due to the narrowness of the area, which is in agreement with studies such as [53] and [86].

The lowest one is Lavan (0.96 m) located on the northeast of PG (Station 11, Figure 2). The northwest and northeast side of PG evokes a kind of mirror image in the mind in terms of tidal mean levels.

Figure 3 represents the comparisons of 17 stations for the first solar month of 2018 (January 1, 2018-January 31, 2018). Full moon was on 2 and 31 and new moon was 17 of January 2018 during this month. As it is obvious, tidal heights of stations, located on OG, are approximately small. The SH tidal ranges are higher. PG shows different styles. On the northeast, tidal ranges are very small (Table 3), but it becomes higher as it travels into the head of PG and it reaches to the highest value on the 17th station, Emam Khomeini Port (5.151 m).

Table 3. Tidal stations of the study along the north coasts of OG, SH and PG.

Basin	Station No. and Name	Min. (m)	Max. (m)	Range (m)
Oman Gulf (OG)	St. 1 Chabahar	-0.236	2.896	3.132
	St. 2 Konarak	-0.022	3.065	3.087
	St. 3 Bandzak	0.045	3.959	3.914
	St. 4 Larak	0.072	3.222	3.15
Strait of Hormuz (SH)	St.5 Bahman Port	-0.180	3.588	3.768
	St. 6 Shahid Rajae Port	-0.159	3.951	4.11
	St. 7 Pol Port	-0.075	4.526	4.601
	St. 8 Khamir Port	-0.185	4.578	4.763
	St. 9 Lengeh Port	0.011	2.629	2.618
North-East	St. 10 Charak Port	0.107	2.200	2.093
	St. 11 Lavan	0.047	1.744	1.697
Persian Gulf (PG)	St. 12 Taheri	-0.027	1.953	1.98
	St. 13 Ameri Port	0.285	2.264	1.979
North-West	St. 14 Bushehr	0.133	2.214	2.081
	St. 15 Genaveh Port	0.303	2.701	2.398
	St. 16 Butaheri	-0.039	3.313	3.352
	St. 17 Emam Khomeini Port	-0.176	4.975	5.151

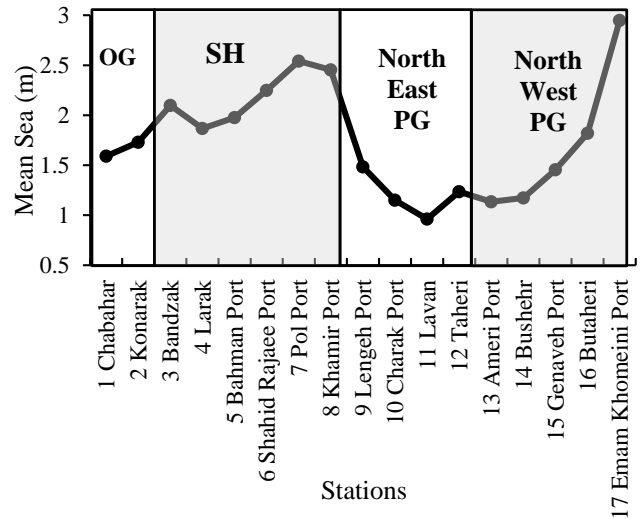


Figure 2. The Mean Level of each Station (January 1, 2014 to December 31, 2018) calculated by tidal data [58].

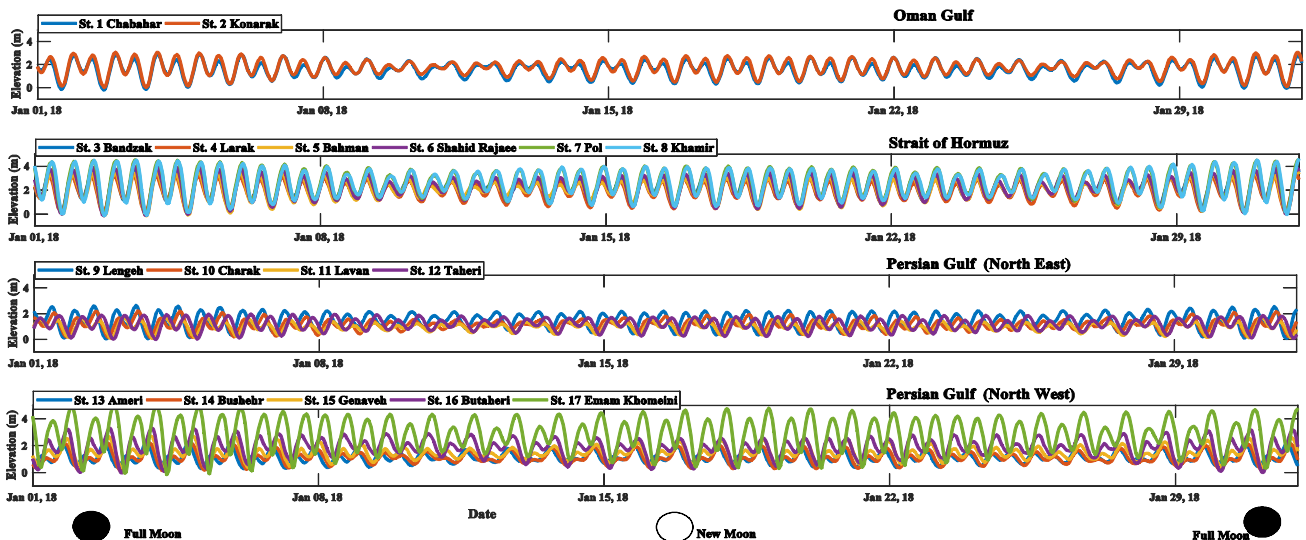


Figure 3. Tides in January 1, 2018 to January 31, 2018. The tide information was achieved by [58], with 30 minutes' interval.

The results of a one-year (2018) t-tide analysis from the Iran National Cartographic Center, Water Management and Tidal Affairs [58] and the predicted t-tide [69] tides by 61 tidal constituents have been prepared for seven random stations (Chabahar, Larak, Khamir Port,

Lengeh Port, Taheri, Bushehr and Emam Khomeini Port) located on OG, SH and PG on Figure 4. It is obvious that the two-time series (the original time series and the predicted one by 61 constituents) have small differences.

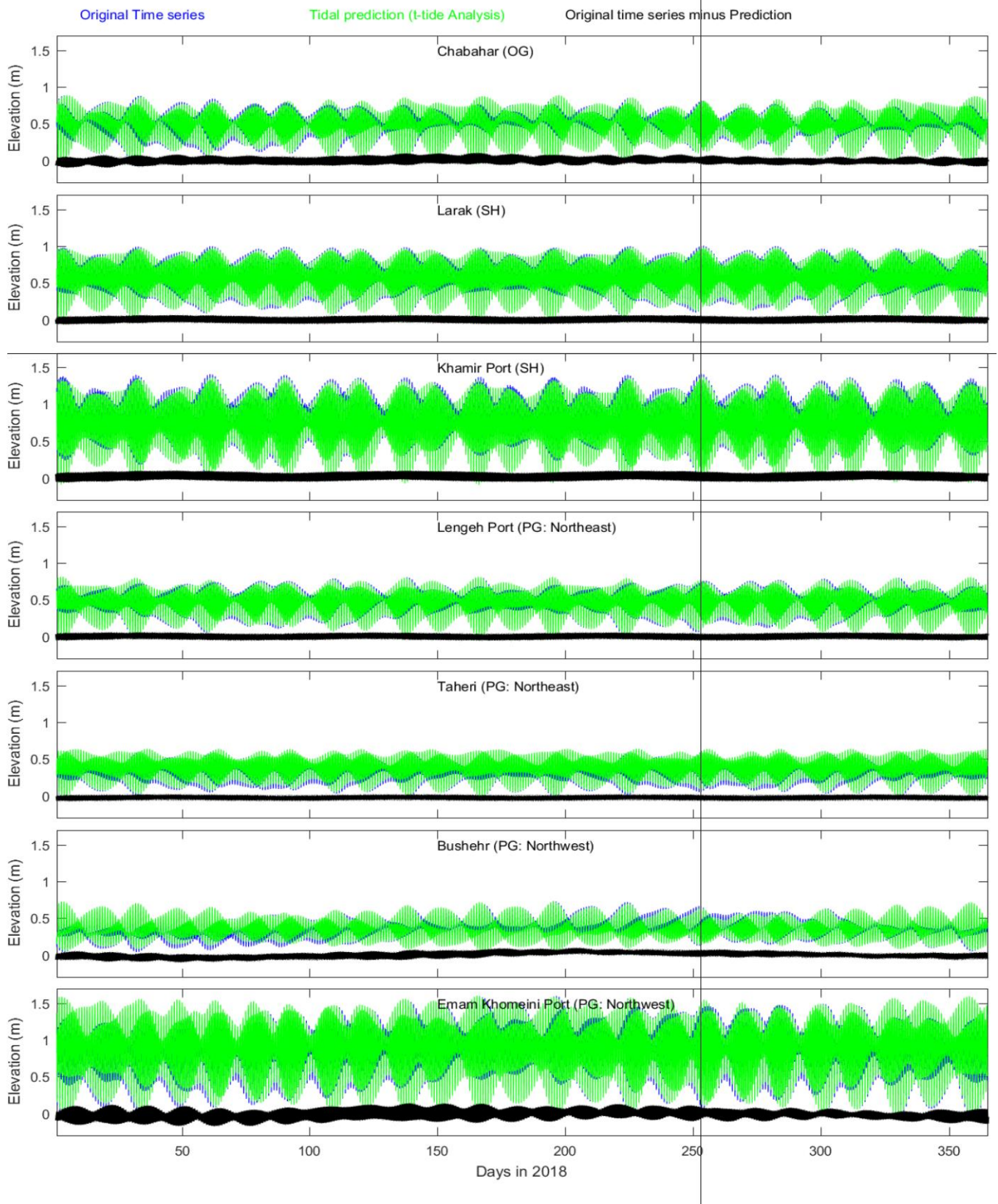


Figure 4. The original (blue) and predictional (green) tidal amplitudes (in meters) and their differences (origin-prediction) (black) for Chabahar (located on OG), Larak and Khamir Port (located on SH), Lengeh Port and Taheri (located on the northeast of PG), Bushehr and Emam Khomeini Port (located on the northwest of PG) for 2018.

The difference between the actual tide and the predicted tide in all stations is less than 0.2 meters. This difference is even less than 0.1 meters in stations like Lark, Langeh Port, Taheri and Bushehr. Comparing Figure 2 and Figure 4 shows that the water level of these stations are insignificant. In a station like Emam Khomeini Port, which has a significant tidal range, the predicted tide with 61 components has a significant

error, and therefore, more components should be considered in the construction of Emam Khomeini tides especially in spring tides.

3.2. The tidal constituents

Amplitude of each tidal constituent are provided on Figure 5. The important point of Figure 5 is the discreteness of the frequency of the components, which is acceptable in the characteristics of tides.

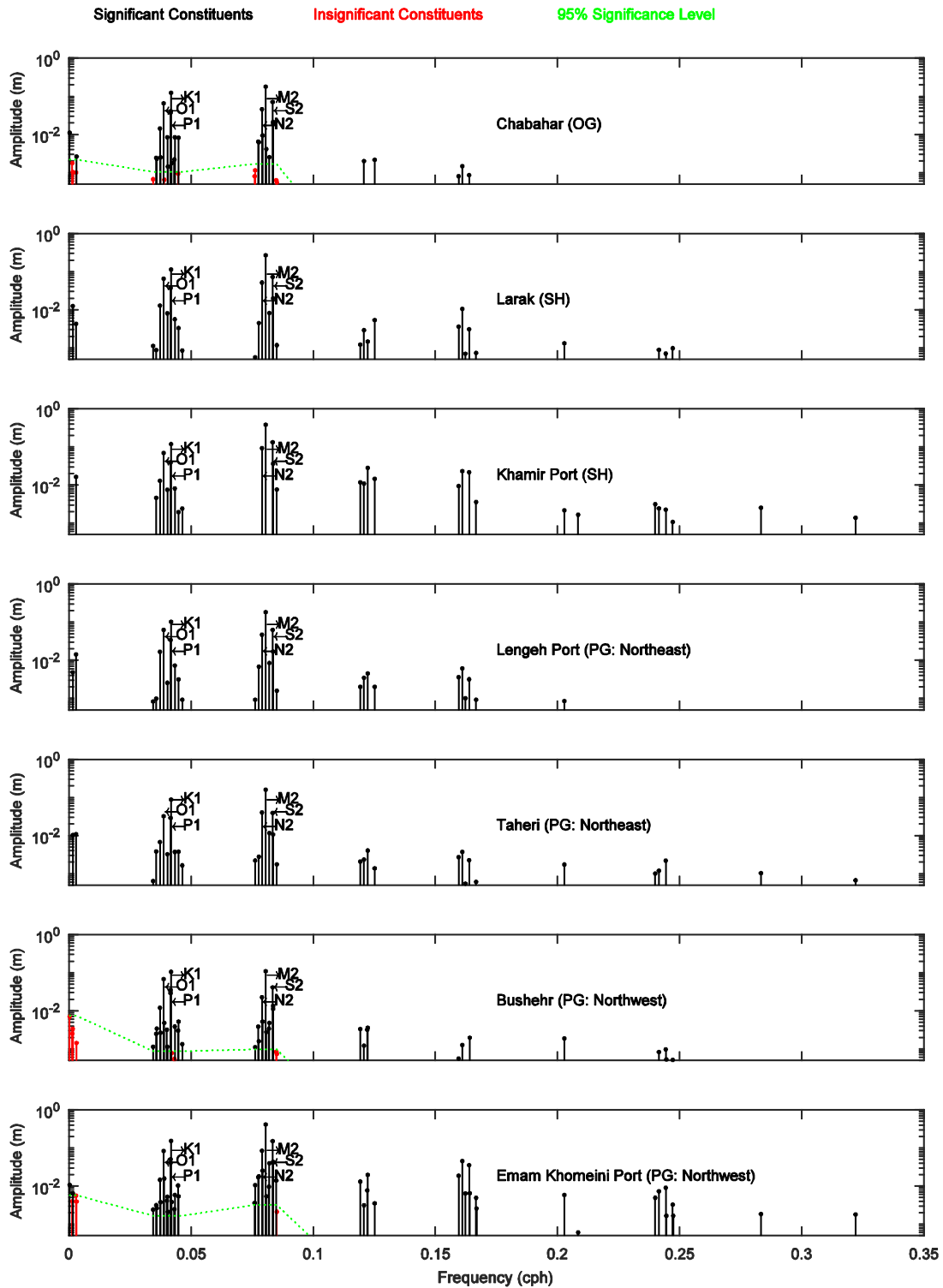


Figure 5. The predicted components of the selected station for Chabahar (located on OG), Larak and Khamir Port (located on SH), Langeh Port and Taheri (located on the northeast of PG), Bushehr and Emam Khomeini Port (located on the northwest of PG) by tide library for 2018.

By the comparison of stations, it can be clearly seen that the tidal components in different stations do not have the same values and their types may also differ from one station to another. The main components (K_1 , O_1 , P_1 , M_2 , S_2 , and N_2) with a frequency less than 0.1 cph in all stations are of the order greater than 10^{-2} m. Components with a frequency of more than 0.2 cph are variable in each station and some components may not be seen in some stations in even the order less than 10^{-2} m.

Table 4 shows the first ten tidal components at each station. It can be seen that the tidal components M_2 , S_2 , K_1 , and O_1 are the top four components in ten stations. There are also seven exception stations that are related to SH and PG. In the Bandzak, Shahid Rajaei Port, Pol Port and Khamir Port stations on SH, the O_1 component is less important than the N_2 component, and N_2 occupies the fourth rank in the components. In the northeast of the PG, the N_2 component reaches the third level of importance at Taheri station. In the northwest of PG, in Emam Khomeini Port station (station 17), the N_2 component has the fourth position and the O_1 component has the fifth position. In Butahari port (station 16), component S_2 ranks fifth, and components M_2 , K_1 , O_1 , and N_2 occupy the positions of the first to fourth ranks, respectively.

These exception stations go back to SH and northwest of PG, which shows the importance of the bending of SH and the shallowing of the northwest of PG. Emami et al., (2019) showed that the shape of the coastline is effective in the tidal pattern [86]. This study confirm that the type of tidal component is different, especially in SH because of its bend which is in agreement with [87].

From the fifth to the tenth component, there are many changes in the type of important components' rank (Table 4). The top ten components of stations include 21 components in total. If we consider these 21

components, the importance of the components changes again.

Figure 6 shows the classification of stations according to the region and type of importance. It can be seen that some of the components are not prioritized in some stations, so the investigation of one station can be different from another station and cannot be generalized.

In many ports of the world, the tide is non-linear and many other components of the tide become important. On the head of PG, it can be seen that the tidal waves in Emam Khomeini port (Station 17) are very sharp (Table 3 and Figure 6) due to the shallowing of the area and after the M_2 and K_1 components, the semi-diurnal S_2 and N_2 components are stronger than the diurnal components of O_1 and P_1 (Table 4). Other components of the order of seven to ten are also semidiurnal or quarterdiurnal. In extreme cases, the incoming waves steepens so much the leading edge is nearly vertical, and the wave propagates as solitary wave and can form a tidal bore. These tides steepen and become non-linear.

The calculated t-tide amplitudes of four major semidiurnal (M_2 , S_2) and diurnal (O_1 , K_1) constituents (as reported by [1, 21-22]) is shown on Figure 6. At some stations (Bandzak, Shahid Rajaei Port, Pol Port, Khamir Port, Taheri, Ameri Port, Bushehr, Butaheri and Emam Khomeini Port), one of these constituents is missing as the four top tidal constituents.

3.3. F factor

Figure 7 also shows the form factor, F, according to Eq. 2, for the stations. The comparison of Table 2 and Figure 7 clearly shows that in no station the F factor is greater than 1.5 m and none of them are less than 0.25, therefore, therefore, all the studied stations on Iranian coasts are mainly mixed semidiurnal tides.

Table 4. The first 10 top tidal constituents achieved by the tidal analysis of 2018 for stations by at-tide along the north coasts of OG, SH and PG

Basin	No. Stations Names	Order of Importance										
		1	2	3	4	5	6	7	8	9	10	
Oman Gulf (OG)	1 Chabahar	M2	K1	S2	O1	N2	P1	K2	Q1	SSA	NU2	
	2 Konarak	M2	K1	S2	O1	N2	P1	K2	NO1	Q1	MU2	
Strait of Hormuz (SH)	3 Bandzak	M2	K1	S2	N2	O1	P1	K2	MU2	ETA2	Q1	
	4 Larak	M2	K1	S2	O1	N2	P1	K2	Q1	MM	M4	
	5 Bahman Port	M2	K1	S2	O1	N2	P1	J1	K2	Q1	MSF	
	6 Shahid Rajaei Port	M2	S2	K1	N2	O1	P1	K2	NU2	Q1	L2	
	7 Pol Port	M2	K1	S2	N2	O1	P1	K2	MK3	M4	Q1	
	8 Khamir Port	M2	S2	K1	N2	O1	P1	K2	MK3	M4	MS4	
Persian Gulf (PG)	9 Lengeh Port	M2	K1	O1	S2	N2	P1	K2	Q1	MSF	L2	
	North East	10 Charak Port	M2	K1	O1	S2	N2	P1	MSF	NO1	Q1	K2
		11 Lavan	M2	K1	O1	S2	P1	N2	K2	MSF	Q1	NO1
		12 Taheri	M2	K1	N2	S2	O1	P1	L2	MSF	K2	MM
		13 Ameri Port	M2	K1	O1	S2	P1	N2	MSF	Q1	K2	OO1
	North West	14 Bushehr	M2	K1	O1	S2	P1	N2	K2	Q1	SSA	OO1
		15 Genaveh Port	M2	K1	O1	S2	P1	N2	NO1	MSF	K2	MK3
	16 Butaheri	M2	K1	O1	N2	S2	P1	MSF	MM	Q1	MK3	
	17 Emam Khomeini Port	M2	K1	S2	N2	O1	P1	M4	K2	L2	MS4	

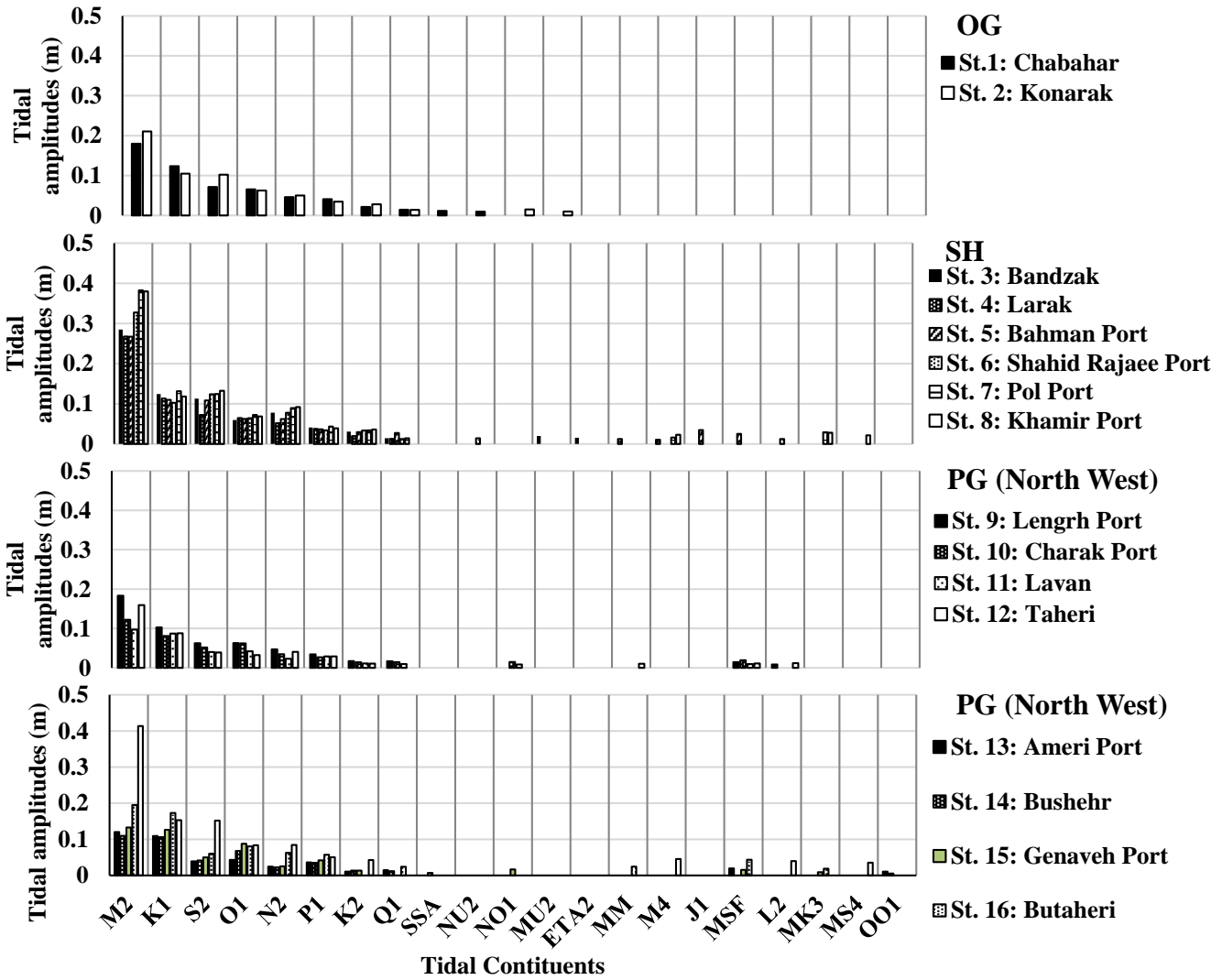


Figure 6. The amplitudes (in meters) of the first major tidal constituents achieved by the analysis of 2018 data of t-tide for all stations.

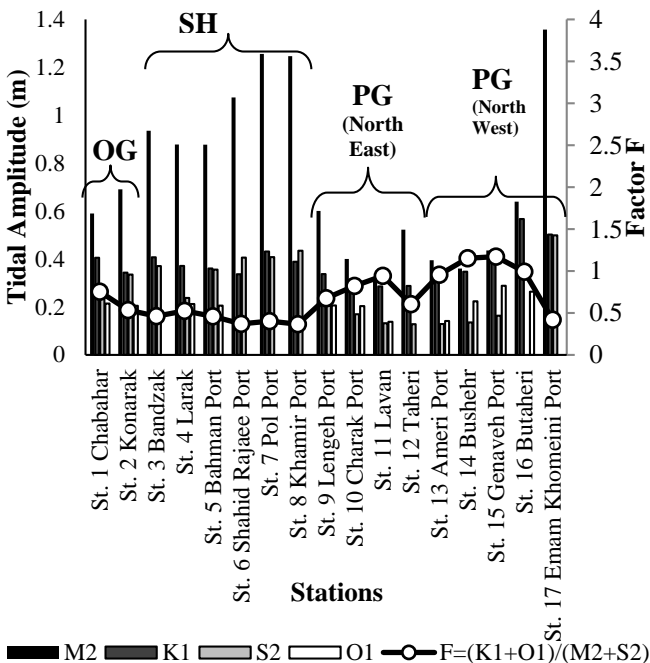


Figure 7. (Left axis:) The tidal calculated amplitudes of four major semidiurnal (M_2 , S_2) and diurnal (O_1 , K_1) constituents as reported by different researches [1, 21-22] by t-tide. (Right axis:) The form factor, F , (Eq. 2), calculated by M_2 , S_2 , O_1 and K_1 without consideration the rank of importance of that tidal constituents.

5. Conclusions

The body forces act directly on deep oceanic waters, but not directly in coastal regions. In open ocean, the tidal range is less than one meter. At the entrance opening of special points such as gently sloping surfaces, funnel-like or chimney-like surfaces is higher due to the reflection of the wave and its Refraction. The tidal range can be enhanced in funnel-like or chimney-like surfaces due to the shape of the coastline and the narrowness of the entrance opening. In this study, two areas with different appearances have been examined via tides. Persian Gulf (PG) connects Oman Gulf (OG) through the Strait of Hormuz (SH) as a narrow funnel-like shape.

Results show that the range and components of harmonic astronomical components are strongly influenced by local geography especially on SH and PG. On the head of PG, tides are strong because tides propagate into very shallow water e.g. river estuary. Tides steepen and become non-linear. Emam Khomainei Port is a good example of the shallow water condition because of the estuary of Khur-e-Mousa. Semidiurnal tides are very important components on this station.

Contrary to the studies mentioned four important tidal components are M_2 , S_2 , K_1 and O_1 on PG, this study clearly showed that in the stations like Bandazk, Shahid Rajaei Port, Pol Port, Khamir Port, Taheri, and Imam Khomeini Port, the N_2 component is more important than the O_1 component. Except for the M_2 component, which is the most important component of all studied area, the order of importance of other components changes on the stations. This issue is related to the geographical changes of the region in terms of appearance shape or depth. Further studies regarding the wave reflection by the coastline which is effective in increasing the range, or the rotation of the tidal waves in the mouth of the strait which increases the energy of the tidal wave, or atmospheric effects such as wind, pressure and precipitation is recommended.

List of Major Symbols

F	Form Factor
K_1	Lunar-Solar, diurnal
K_2	Lunar-Solar, semidiurnal
M_2	Main Lunar, semidiurnal
N_2	Lunar elliptic, semidiurnal
O_1	Main Lunar, diurnal
P_1	Main Solar, diurnal
S_2	Main Solar, semidiurnal

8. References

- [1] Reynolds, R.M., (1993). *Physical oceanography of the Gulf, Strait of Hormuz, and the Gulf of Oman—Results from the Mt Mitchell expedition*, Marine Pollution Bulletin, Vol.27, p.35-59. DOI: 10.1016/0025-326x(93)90007-7
- [2] Cartwright, D.E., and Tayler, R.J., (1971), *New computations of the tide-generating potential*, Geophysical Journal of the Royal Astronomical Society, Vol.23(1), p.45-74, DOI: 10.1111/j.1365-246X.1971.tb01803.x
- [3] Darwin, G.H., (1911), *The Tides and Kindred Phenomena in the solar system*, Nature, Vol. 88(2193), p.35-36. DOI: 10.1038/088035a0
- [4] Symon, K.R., (1971), *Mechanics addison-wesley*. Reading, MA, 1.
- [5] Pond, S. and Pickard, G.L., (1983), *Introductory dynamic oceanography*, 2nd Edition, Pergamon Press.
- [6] Hammons, T.J., (1993), Tidal power. Proceedings of the IEEE, Vol.81(3), p.419-433. DOI: 10.1109/5.241486
- [7] Bryden, I.G. and Macfarlane, D.M., (2000), *The utilisation of short term energy storage with tidal current generation systems*. Energy, Vol.25(9), p.893-907. DOI: 10.1016/s0360-5442(00)00020-7
- [8] Doodson, A.T., (1922), *Harmonic development of the tide-generating potential*. Proceedings of the Royal Society of London, Series A, Vol.100(704), p.305–329. DOI: 10.1098/rspa.1921.0088
- [9] SHOM and UKHO, (2017), *Tidal Constituents*, Date modified May 8, 2017. Retrieved August 12, 2018, from https://www.iho.int/mtg_docs/com_wg/IHOTC/IHOTC_Misc/TWCWG_Constituent_list.pdf.
- [10] Woodworth, P.L., (2010), *A survey of recent changes in the main components of the ocean tide*, Continental Shelf Research, Vol.30(15), p.1680-1691. DOI: 10.1016/j.csr.2010.07.002
- [11] Müller, M., Arbic, B.K. and Mitrovica J., (2011), *Secular trends in ocean tides: observations and model results*. Journal of Geophysical Research, Vol.116(C05) p.013. DOI: 10.1029/2010jc006387
- [12] Haigh, I.D., Wijeratne, E.M.S., MacPherson, L.R., Pattiaratchi, C.B., Mason, M.S., Crompton, R.P. and George S., (2014), *Estimating present day extreme water level exceedance probabilities around the coastline of Australia: tides, extra-tropical storm surges and mean sea level*, Climate Dynamics, Vol.42(1-2), p.121-138. DOI: 10.1007/s00382-012-1652-1
- [13] Mawdsley, R.J., Haigh, I.D. and Wells N.C., (2015), *Global changes in tidal high water, low water and range*. Earth's Futures, Vol.3(2), p.66-81. DOI: 10.1002/2014ef000282
- [14] Jay, D.A., (2009), *Evolution of tidal amplitudes in the eastern Pacific Ocean*, Geophysical Research Letters, Vol.36(4), p.L04603, DOI: 10.1029/2008gl036185
- [15] Ray, R.D., (2006), *Secular changes of the M2 tide in the Gulf of Maine*, Continental Shelf Research, Vol.26(3), p.422-427, DOI: 10.1016/j.csr.2005.12.005
- [16] Ray, R. D. (2009), *Secular changes in the solar semidiurnal tide of the Western North Atlantic Ocean*, Geophysical Research Letters, Vol.36(19), p.L19601, DOI: 10.1029/2009gl040217
- [17] Müller, M., (2011), *Rapid change in semi-diurnal tides in the North Atlantic since 1980*. Geophysical Research Letters, 38(11), p. L11602. DOI: 10.1029/2011gl047312
- [18] Feng, X., Tsimplis, M.N. and Woodworth, P.L., (2015), *Nodal variations and long-term changes in the main tides on the coasts of China*. Journal of Geophysical Research: Oceans, Vol.120(2), p.1215-1232. DOI: 10.1002/2014jc010312
- [19] Feng, X., and Tsimplis, M.N., (2014), *Sea level extremes at the coasts of China*, Journal of Geophysical Research: Oceans, Vol.119(3), p.1593–1608, DOI: 10.1002/2013jc009607
- [20] Rasheed, A. S., and Chua, V.P., (2014), *Secular trends in tidal parameters along the coast of Japan*. Atmosphere-Ocean, Vol.52(2), p.155-168. DOI: 10.1080/07055900.2014.886031

- [21] Pous, S., Carton, X. and Lazure, P., (2012), *A Process Study of the Tidal Circulation in the Persian Gulf*, Open Journal of Marine Science, Vol.2(04), p.131-140. DOI: 10.4236/ojms.2012.24016
- [22] Akbari, P., Sadrinasab, M., Chegini, V., Siadatmousavi, M., (2016), *Tidal constituents in the Persian Gulf, Gulf of Oman and Arabian Sea: a numerical study*, Indian Journal of Geo-Marine Sciences, Vol.45(8), p.1010-1016.
- [23] ESRI, (2011), *ArcGIS Desktop*, 64-bit, Version 10.3, Released 2011, Redlands, CA: Environmental Systems Research Institute.
- [24] Randall, J.E., (1995), *Coastal fishes of Oman*, University of Hawaii Press- Hawaii.
- [25] Barth, H.J. and Khan, N.Y., (2008), *Biogeophysical setting of the Gulf*, Protecting the Gulf's marine ecosystems from pollution, p. 1-21. DOI: 10.1007/978-3-7643-7947-6_1
- [26] Nadim, F., Bagtzoglou, A.C. and Iranmahboob, J., (2008), *Coastal management in the Persian Gulf region within the framework of the ROPME programme of action*. Ocean and Coastal Management, Vol.51(7), p.556-565. DOI: 10.1016/j.ocecoaman.2008.04.007
- [27] Barth, H.-J. (1998). *Sebkhas als Ausdruck von Landschaftsdegradation im zentralen Küstentiefland der Ostprovinz Saudi-Arabiens*. Regensburger Geographische Schriften-Regensburg.
- [28] Sugden, W., (1963), *The hydrography of the Persian Gulf and its significance in respect to evaporative deposition*. American Journal of Science, Vol.261(8), p.741–55. DOI: 10.2475/ajs.261.8.741
- [29] Johns, W.E., Yao, F., Olson, D.B., Josey, S.A., Grist, J.P. and Smeed, D.A., (2003), *Observations of seasonal exchange through the Straits of Hormuz and the inferred freshwater budgets of the Persian Gulf*, Journal of Geophysical Research, Vol.108(C12), p.3391. DOI: 10.1029/2003jc001881
- [30] Privett, D.W. (1959), *Monthly charts of evaporation from the North Indian Ocean, including the Red Sea and the Persian Gulf*, Quarterly Journal of the Royal Meteorological Society, Vol.85(366), p.424–428. DOI: 10.1002/qj.49708536614
- [31] Hastenrath, S. and Lamb, P.J., (1979). *Climatic atlas of the Indian Ocean*, Part 2, The ocean heat budget, University of Wisconsin Press, Madison-Wisconsin.
- [32] Brewer, P.G. and Dyrssen, D., (1985), *Chemical Oceanography of the Persian Gulf*, Progress in Oceanography, Vol.14, p.41–55. DOI: 10.1016/0079-6611(85)90004-7
- [33] Ahmad, F. and Sultan, S.A.R., (1991), *Annual mean surface heat fluxes in the Arabian Gulf and the net heat transport through the Strait of Hormuz*, Atmosphere-Ocean, Vol.29(1), p.54–61. DOI: 10.1080/07055900.1991.9649392
- [34] Soyuf Jahromi, M., (2022), *The spatial and temporal monitoring of the sea surface temperature anomaly of the Strait of Hormuz*. International Journal Of Coastal, Offshore And Environmental Engineering (ijcoe), Vol.7(4), p.1-6. DOI: 10.22034/ijcoe.2022.164980
- [35] Pourkarimian, A., Soyuf Jahromi, M., and Malakooti, H. (2021). *Tracking of the oceanic water content resources of the precipitation in Dayyer Port (March 2017)*. Journal of Marine Science and Technology, Vol.20(3), p.31-49. DOI: 10.22113/jmst.2019.182862.2282
- [36] Pourkarimian, A., Soyuf Jahromi, M., and Malakooti, H. (2022). *Investigation and study of flood moisture transfer (Case study: March 2017 in south and southwest of Iran)*. Amphibious Science and Technology, Vol.2(4), p.40-61. DOI: 10.22034/jamst.2022.543537.1050
- [37] Swift, S.A. and Bower, A.S., (2003), *Formation and circulation of dense water in the Persian/Arabian Gulf*, Journal of Geophysical Research, Vol.108(C1), p.3004, DOI: 10.1029/2002jc001360
- [38] Darskhan, S. and Soyuf Jahromi, M., (2022) *Numerical solution of the geostrophic mesoscale eddy in the shallow water model*, Journal of Oceanography, Vol.13(49), p.81-91, (In Persian) DOI: 10.52547/joc.13.49.81
- [39] Ramak, H., Soyuf Jahromi, M. and Akbari, P., (2021), *Using surface temperature data of the Oman Sea to identify subsurface water of the Persian Gulf*, Hydrophysics, Vol.7(2), p.79-93. (In Persian)
- [40] Ramak, H., Soyuf Jahromi, M. and Akbari, P., (2022a), *Persian Gulf Water mass tracking by surface temperature and salinity properties*, Journal of Oceanography, Vol.12(48), p.13-28. (In Persian) DOI: 10.52547/joc.12.48.13
- [41] Ramak, H., Soyuf Jahromi, M. and Akbari, P., (2022b), *Persian Gulf Water mass tracking by surface temperature and salinity properties*, Journal of Oceanography, Vol.12(48), p.13-28. (In Persian) DOI: 10.52547/joc.12.48.13
- [42] Ramak, H., Soyuf Jahromi, M. and Akbari, P., (2023a) *Investigating the downwelling of Persian Gulf Water in the Gulf of Oman*. International Journal Of Coastal, Offshore And Environmental Engineering (ijcoe), Vol.8(1), p.1-9. DOI: 10.22034/ijcoe.2023.166317
- [43] Ramak, H., Soyuf Jahromi, M. and Akbari, P., (2023b), *Investigation of salinity and temperature of Persian Gulf water by FVCOM Model*. Journal of Oceanography, Vol.13 (52), p.106-120, (In Persian) DOI: 10.52547/joc.13.52.8
- [44] Lashkari, S., Soyuf Jahromi, M., and Hamzei, S., (2023), *Seasonal changes of the Persian Gulf water mass in the Gulf of Oman*. Journal of Oceanography,

- 14 (53) :103-122, (In Persian) DOI: 10.52547/joc.14.53.9
- [45] ROPME, 2004. *State of the Marine Environment Report, 003*. The Regional Organization for the Protection of the Marine Environment (ROPME)-Kuwait, p.217.
- [46] Soyuf Jahromi, M., Sadrinasab, M. Aliakbari Bidokhti, A.A., (2014), *3D simulation of measured Oman data at late winter, 2005*. Journal of Marine Science and Technology, Vol.13(3), p.21-31. (In Persian), DOI: 10.22113/jmst.2014.7821
- [47] Lashkari, S., Soyuf Jahromi, M., and Hamzei, S., (2022), *The temperature changes of WOA data in upper layers of Gulf of Oman*. 1st international marine science conference with the approach of innovation in aquatic ecosystems based on sea-based economy, p.383-395. (In Persian)
- [48] Al-Majed, N. and Preston, M., (2000), *An assessment of the total and methyl mercury content of zooplankton and fish species tissue collected from Kuwait territorial waters*. Marine Pollution Bulletin, Vol.40(4), p.298–307. DOI: 10.1016/s0025-326x(99)00217-9
- [49] Mohammadpour, F., Soyuf Jahromi, M., and Hamzei, S., (2022), *Comparison of the vertical temperature distribution on the east of the strait of Hormuz*. 1st international marine science conference with the approach of innovation in aquatic ecosystems based on sea-based economy, p.176-188. (In Persian)
- [50] Mohammadpour, F., Soyuf Jahromi, M. and Hamzei, S., (2023), *Winter study of the stability and Double diffusion convection in the east of the Strait of Hormuz*, Hydrophysics, Vol.8(2), p.79-93. (In Persian)
- [51] Defant A., (1960), *Physical Oceanography*, (Pergamon Press LTD) Vol. 2, p. 571.
- [52] Hunter, J.R., (1982), *The physical oceanography of the Arabian Gulf: a review and theoretical interpretation of previous observations*. 1st Arabian Gulf conference on marine environment and pollution. Kuwait University, Faculty of Science, Kuwait, p. 1-23.
- [53] Soyuf Jahromi, M. and Emami, M., (2021), *The role of different positions of tidal turbines for energy extraction in Qeshm channel*. International Journal Of Coastal, Offshore And Environmental Engineering (ijcoe), Vol.6(5), p.1-9. DOI: 10.22034/ijcoe.2021.152602.
- [54] Lehr, W.J., (1984), *A brief survey of oceanographic modelling and oil spill studies in the KAP region*. NESCO Reports in Marine Science, Vol.28, p.4–11.
- [55] Najafi, H.S. (1979), *Modelling tides in the Persian Gulf using dynamic nesting*, PhD thesis, University of Adelaide, Adelaide, South Australia.
- [56] Lardner, R.W., Belen, M.S. and Cekirge. H.M., (1982), *Finite difference model for tidal flows in the Arabian Gulf*. Computers & Mathematics with Applications, Vol.8(6), p.425–444. DOI: 10.1016/0898-1221(82)90018-9
- [57] Teubner, M.D., Najafi, H.S., Noye, B.J. and Rasser, P.E., (1999), *Modelling tides in the Persian Gulf using dynamic nesting*, Modelling Coastal Sea Processes, p.57-80. DOI: 10.1142/9789814350730_0003
- [58] <http://iranhydrography.ncc.org.ir>
- [59] Bowen, A.J., (1972), *The tidal regime of the River Thames; long-term trends and their possible causes*, Philosophical Transactions of the Royal Society of London, Series A: Mathematical, Physical and Engineering Sciences, Vol.272(1221), p.187-199. DOI: 10.1098/rsta.1972.0045
- [60] Amin, M., (1983), *On perturbations of harmonic constants in the Thames Estuary*. Geophysical Journal International, Vol.73(3), p.587-603. DOI: 10.1111/j.1365-246x.1983.tb03334.x
- [61] Jay, D.A., Leffler, K. and Degens, S., (2011), *Long-term evolution of Columbia River tides*, Journal of Waterway, Port, Coastal, and Ocean Engineering, Vol.137(4), p.182-191. DOI: 10.1061/(asce)ww.1943-5460.0000082
- [62] Vellinga, N.E., Hoitink, A.J.F., van der Vegt, M., Zhang, W. and Hoekstra, P., (2014), *Human impacts on tides overwhelm the effect of sea level rise on extreme water levels in the Rhine–Meuse delta*, Coastal Engineering, Vol.90, p.40–50. DOI: 10.1016/j.coastaleng.2014.04.005
- [63] Chernetsky, A.S., Schuttelaars, H.M. and Talke, S.A., (2010), *The effect of tidal asymmetry and temporal settling lag on sediment trapping in tidal estuaries*. Ocean Dynamics, Vol.60(5), p.1219-1241. DOI: 10.1007/s10236-010-0329-8
- [64] Familkhalili, R. and Talke S.A., (2016), *The Effect of Channel Deepening on Storm Surge: Case Study of Wilmington, NC*, Geophysical Research Letters, Vol.43(17), p.9138-9147. DOI: 10.1002/2016gl069494
- [65] Colossi, J.A. and Munk, W., (2006), *Tales of the Venerable Honolulu Tide Gauge*, Journal of Physical Oceanography, Vol.36(6), p.967–996, DOI: 10.1175/jpo2876.1
- [66] Müller, M., Cherniawsky, J.Y., Foreman, M.G.G. and Storch J.S. (2012), *Global M2 internal tide and its seasonal variability from high resolution ocean circulation and tide modeling*. Geophysical Research Letters, Vol.39(19), p.L19607. DOI: 10.1029/2012gl053320
- [67] Forrester, W.D., (1983), *Tidal analysis and prediction*, In: Canadian tidal manual. Ottawa, Ont. Department of Fisheries and Oceans, Canada, p.39-54.
- [68] Pawlowicz, R., (2002), *Observations and linear analysis of sill-generated internal tides and estuarine flow in Haro Strait*, Journal of Geophysical Research: Oceans, Vol.107(C6), p.9-1. DOI: 10.1029/2000jc000504

- [69] Pawlowicz, R., Beardsley, B. and Lentz, S., (2002), *Classical tidal harmonic analysis including error estimates in MATLAB using T_TIDE*. Computers and Geosciences, Vol.28(8), p.929-937. DOI: 10.1016/s0098-3004(02)00013-4
- [70] http://www.eos.ubc.ca/~rich/t_tide/t_tide_v1.3beta.zip
- [71] Desyari, M., (2019), *Analisis Karakteristik Pasang Surut Perairan Dermaga Tempat Pelelangan Ikan (TPI) Palopo Sulawesi Selatan dengan Menggunakan Metode Admiralty, T-Tide, TMD, dan NAOTide*, PhD thesis, Universitas Brawijaya-Brawijaya.
- [72] Hennon, T.D., Alford, M.H. and Zhao, Z., (2019), *Global assessment of semidiurnal internal tide aliasing in Argo profiles*. Journal of Physical Oceanography, Vol.49(10), p.2523-2533. DOI: 10.1175/jpo-d-19-0121.1.
- [73] Suharyo, O. S., Setiadi, J., Sukoco, N. B., & Kuncoro, K. (2020). *The analysis formulation of the Lowest Astronomical Tide (LAT) based on the time observation (The case study of Benoa Waters)*. Journal ASRO, Vol.11(1), p.77-87. DOI: 10.37875/asro.v11i1.205
- [74] Marques, O.B., Alford, M.H., Pinkel, R., MacKinnon, J.A., Klymak, J.M., Nash, J.D., Waterhouse, A.F., Kelly S.M., Simmons, H.L. and Braznikov, D., (2021), *Internal tide structure and temporal variability on the reflective continental slope of Southeastern Tasmania*. Journal of Physical Oceanography, Vol.51(2), p.611-631. DOI: 10.1175/jpo-d-20-0044.1
- [75] Wan, Y., (2023), *Harmonic analysis in tide analysis*. 2nd International Conference on Statistics, Applied Mathematics, and Computing Science (CSAMCS 2022), Vol.12597, p.768-774.
- [76] The MathWorks Inc. (2016), *MATLAB and Statistics Toolbox 64-bit*, Version 2016a, Release 2016a, Natick, Massachusetts, USA.
- [77] Foremann, M., (1977). *Manual for tidal heights analysis and prediction*, Pacific marine science report, Vol.10, p.66-77.
- [78] Stal, C., Poppe, H., Vandenbulcke, A. and De Wulf, A., (2016), *Study of post-processed GNSS measurements for tidal analysis in the Belgian North Sea*. Ocean Engineering, Vol.118, p.165-172. DOI: 10.1016/j.oceaneng.2016.04.014
- [79] Lin, H., Hu, J., Zhu, J., Cheng, P., Chen, Z., Sun, Z., and Chen, D., (2017), *Tide-and wind-driven variability of water level in Sansha Bay, Fujian, China*. Frontiers of Earth Science, Vol.11(2), p.332-346. DOI: 10.1007/s11707-016-0588-x
- [80] Soyuf Jahromi, M. and Shahmansoori, Z. (2021), *The monthly sea-level anomaly patterns on the Persian Gulf*. Iranian journal of Marine technology, Vol.7(4), p.97-106. (In Persian)
- [81] Soyuf Jahromi, M. and Shahmansoori, Z. (2022), *The seasonal changes of sea-level anomalies on the Persian Gulf (1993-2017)*. Journal of Marine Science and Technology, Vol.21(1), p.1-15. (In Persian) DOI: 10.22113/jmst.2021.197166.2303
- [82] Lisitzin, E., (1974), *Sea-level changes*: Elsevier Oceanography Series (Vol. 8).
- [83] Pugh, D., (1987), *Tides, Surges and Mean Sea Level: A Handbook for Engineers and Scientists*. John Wiley & Sons, Chichester.
- [84] Pugh, D., (2004), *Changing Sea Levels-Effects of Tides, Weather and Climate*. Cambridge University Press, Cambridge.
- [85] Yeknami, S.R., Soltanpour, M., and Ranji, Z. (2016). *Analysis of nearshore local effects on tidal behaviour at imam Khomeini port and Musa bay*. Coastal Engineering Proceedings, Vol.(35), p.7-7. DOI: 10.9753/icce.v35.currents.7
- [86] Emami, M., Soyuf Jahromi, M. and Behmanzadegan, A., (2019), *Coastline Effect on Tidal Flow Pattern*. Journal of Marine Science and Technology, Vol.18(2), p.12-25. (In Persian), DOI:0.22113/jmst.2019.122581.2137